Laosuwan, T., Plybour, C., Rotjanakusol, T. (2023): Inspection of burning areas caused by forest fire in doi suthep-pui national park through data obtained from landsat 8 satellite and normalized burn ratio. Agriculture and Forestry, 69 (3): 81-95. doi:10.17707/AgricultForest.69.3.06

DOI: 10.17707/AgricultForest.69.3.06

Teerawong LAOSUWAN[1], Chaiphat PLYBOUR[1], Tanutdech ROTJANAKUSOL*[1]

INSPECTION OF BURNING AREAS CAUSED BY FOREST FIRE IN DOI SUTHEP-PUI NATIONAL PARK THROUGH DATA OBTAINED FROM LANDSAT 8 SATELLITE AND NORMALIZED BURN RATIO

SUMMARY

The objective of this research is to inspect areas burned by a forest fire in Doi Suthep-Pui National Park in Muang District, Chiang Mai Province, Thailand, with data from the Landsat 8 satellite and Normalized Burn Ratio (NBR). The research was conducted by analyzing data from the Landsat 8 satellite between 2017 and 2021 in pre- and postfire periods. Data were analyzed using NBR before analyzing to find burning areas through ΔNBR. The accuracy of results was evaluated point by point using false color composites (7(R),5(G),4(B)) by creating 60 random points. Analysis results revealed that accuracy in the study period was 81.66%, 81.66%, 83.33%, 81.66%, and 86.66%, respectively. Moreover, when inspecting the consistency of analysis results using the Kappa statistic, it was found that, during the study period, the Kappa coefficient was 0.78, 0.81, 0.82, 0.82, and 0.84, respectively. As a result, it could be concluded that false color composites (7(R), 5(G), 4(B)), NBR, and Δ NBR can reliably and consistently be used for specifying areas burned by forest fires. Relevant agencies can apply this case study to inspect further burning areas caused by forest fires.

Keywords: Remote Sensing, Doi Suthep-Pui National Park, Forest Fire, Normalized Burn Ratio, Landsat 8

INTRODUCTION

Forest fire refers to a fire that spreads throughout the natural forest or forestry plantations independently without control. A forest fire cannot be caused if the following three factors, Fire Triangle (Linta *et al.*, 2021), are lacking. There are two fundamental causes of forest fires including (1) natural causes, such as lightning, friction between branches, volcanic eruption, clash of stones, the

[1]Teerawong Laosuwan, Chaiphat Plybour, Tanutdech Rotjanakusol (corresponding author: e-mail: tanutdech.r@msu.ac.th), Department of Physics, Faculty of Science, Mahasarakham University, Maha Sarakham, 44150.THAILAND

Notes: The authors declare that they have no conflicts of interest. Authorship Form signed online.

Recieved:12/03/2023 *Accepted:20/07/2023*

incidence of sunlight to quartz, sunlight shining through water droplets, a chemical reaction in a swamp forest, spontaneous combustion of living creatures) and (2) anthropogenic causes, for example, forest product collection, ignition, and negligence (Ruthamnong, 2019). The rapid population growth increases the need to utilize forest resources; therefore, forests are reclaimed as agricultural and residential areas. The expansion of communities destroys forests rapidly (Department of National Parks, Wildlife and Plant Conservation, n.d.). The remaining forest areas are degenerated and transformed into forests with lower humidity, for example, mixed forests, deciduous forests, and forests with large amounts of grass or meadow that can fuel forest fires (Untamedscience, n.d.).

Furthermore, poverty in rural areas forces people to increasingly rely on forests for living by collecting forest products, hunting wild animals, or clearing forests for farming. These activities require fire, so they become the causes of forest fires. Consequently, the frequency and severity of forest fires are capable natural mechanisms that adjust themselves to balance the forest ecosystem (Urbancreature, 2021; 3armyarea-rta, n.d.). For this reason, forest fires cause severe damage to forests and the environment. Currently, the frequency of forest fires in Thailand has sharply increased, becoming a factor disturbing ecosystem balance. Significant impacts of forest fire are: 1) impact on soil, forest, water, and wild animals as well as small creatures in forests; 2) impact on assets, health, human life, economy, society, and tourism; and 3) impact on global climate (Baankluayonline, 2020). Subsequent impacts cause severe drought in the rainy season, off-season rain, and flooding. As a result, forest fire has become an internationally significant problem that is currently realized by all sectors (Flannigan *et al.,* 2000).

Doi Suthep-Pui National Park has forest and mountain areas. Around 70% of the total area consists of granite mountains and limestone mountains covered by various kinds of forest, including hill evergreen forest, dry evergreen forest, mixed forest, deciduous forest, and deciduous forest mixed with coniferous forest. Forested areas consist of natural forests, forestry plantations, and naturally restored forests (Chiang Mai Provincial Office, 2021). Each year, the number of forests is decreased by 0.02% (Kongmeesup, 2020) due to several causes, mainly deforestation and forest fire. Forest fires impact southern Thailand every year, especially during the dry season from the beginning of November to the end of April (Panyakam & Pongsawat, 2022). Forest fire mainly occurs in mixed forest, deciduous forest, and forestry plantations (Royal Forest Department, n.d.), so it is necessary to build firebreaks in these areas and encourage cooperation with local people regarding forest burning to reduce the severity of forest fire and smoke caused by forest burning (Gnews, n.d.). In addition to data from land surveys, remote sensing technology can be used to evaluate burning forest areas (Boer *et al.,* 2009; Mohammadi *et al.,* 2014; Tariq *et al.,* 2021a and Tariq *et al.*, 2021b).

Currently, remote sensing technology, such as satellite data, is rapidly and efficiently developing (Debbarma and Debnath, 2021; Potić *et al.*, 2021 and Thangaraj and Karthikeyan, 2021). Remote sensing technology contains basic

physics principles on an electromagnetic wave used as media to obtain data without direct contact with objects (ESA, 2016; Elachi and Zyl, 2021; University of Lucknow, n.d.). Moreover, remote sensing technology can record data from vast areas at a lower cost than land surveying (Laosuwan *et al*., 2016; Rotjanakusol and Laosuwan, 2018a; Rotjanakusol and Laosuwan, 2018b; Rotjanakusol and Laosuwan, 2019; Prohmdirek *et al*., 2020; Uttaruk and Laosuwan, 2020; Jomsrekrayom *et al*., 2021, Sangpradid *et al*., 2021; Suriya *et al*., 2021; Uttaruk *et al*., 2022).

MATERIAL AND METHODS

Research area

Doi Suthep-Pui National Park (Figure 1) is located in Muang Chiang Mai District, Mae Rim District, and Hang Dong District, with a total area of 261 km^2 (Thai National Parks, 2023) and consisting of a plentiful forest. Although it is located near Chiang Mai's downtown, most forest areas are on complex mountain ranges, such as Doi Suthep and Doi Pui. The general climate of Doi Suthep-Pui National Park is influenced by southwest monsoon-blowing humidity and clouds causing rain and northeast monsoon blown from China causing coldness and drought.

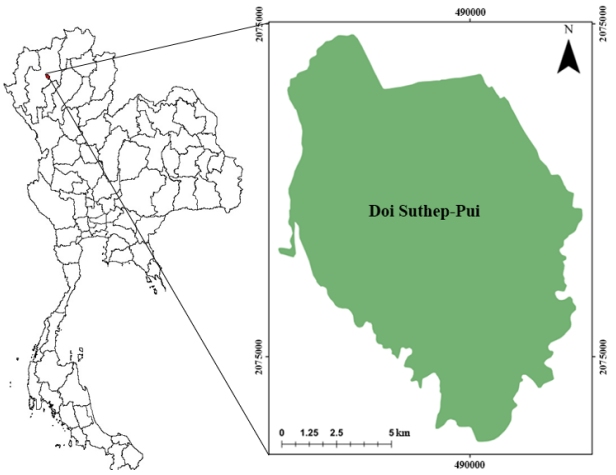

Figure 1. Research area

Satellite Data

The Landsat 8 satellite was launched on May 30th, 2013, under the management of the United State Geological Survey (USGS). It orbits 705 km above the earth's surface with two types of recording devices, including an Operational Land Imager (OLI) (30 m) and a Thermal Infrared Sensor (TIRS) (100 m), and repeats coverage every 16 days. It consists of 11 bands, and the first to seventh and ninth bands consist of wavelengths ranging from 0.43–0.45 μm

(Coastal Aerosol), 0.45–0.51 μm (Blue), 0.53–0.59 μm (Green), 0.64–0.67 μm (Red), 0.85–0.88 μm (Near Infrared: NIR), 1.57–1.65 μm (SWIR 1), 2.11–2.29 μm (SWIR 2), and 1.36–1.38 μm (Cirrus) with a spatial resolution of 30 meters. The eighth band has a wavelength from 0.50–0.68 μm (Panchromatic) with a spatial resolution of 15 m. The tenth and eleventh bands have wavelengths from 10.60–11.19 μm (Thermal Infrared 1, TIRS 1) and 11.50–12.51 μm (TIRS 2) with a spatial resolution of 100 m (USGS, 2022). This research was conducted by analyzing data obtained from the Landsat 8 satellite (https://earthexplorer.usgs.gov/) from December 2017 to 2021 in the pre-fire and from March 2017 to 2021 postfire periods.

Conversion of Digital Number as Reflectance

Conversion of Digital Number as Reflectance is considered the process of data preparation before conducting analysis (pre-processing) by converting Digital Number (DN) obtained from Landsat 8 to Reflectance by using Equation 1 (Ruthamnong, 2019). Subsequently, obtained data were calculated to find adjustments with sun elevation, as shown in Equation 2 (Ruthamnong, 2019).

$$\rho\lambda' = M\rho . Qcal + A\rho \quad (1)$$

Where:

$\rho\lambda'$= TOA planetary reflectance, without correction for solar angle

$M\rho$=Band-specific multiplicative rescaling factor from the metadata (REFLECTANCE_MULT_BAND_x, where x is the band number)

$A\rho$=Band-specific additive rescaling factor from the metadata (REFLECTANCE_ADD_BAND_x, where x is the band number)

Qcal=Quantized and calibrated standard product pixel values (DN)

$$\rho\lambda = (\rho\lambda'/\cos(\theta_{SZ})) = (\rho\lambda'/\sin(\theta_{SE})) \quad (2)$$

Where:

$\rho\lambda$=TOA planetary reflectance

θ_{SE}=Local sun elevation angle. The scene center sun elevation angle in degrees is provided in the metadata (SUN_ELEVATION).

θ_{SZ}=Local solar zenith angle; $\theta_{SZ} = 90° - \theta_{SE}$

Normalized Burn Ratio (NBR) Analysis

NBR is a kind of index designed to find burning areas and evaluate fire severity. This method is similar to the Normalized Difference Vegetation Index (NDVI), but NBR use of the wavelength of Near Infrared (NIR) and Short Wave Infrared (SWIR), as shown in Equation 3 (Keeley, 2009). This method will give plants high Reflectance in Near Infrared (NIR) and low Reflectance in Short Wave Infrared (SWIR). On the other hand, the burning area will have low Reflectance in Near Infrared (NIR) and high Reflectance in Short Wave Infrared

(SWIR). Generally, high NBR indicates a small number of plants, empty spaces, and burning areas. This research analyzed data obtained from Landsat 8 satellite in pre-fire and postfire periods using Normalized Burn Ratio (NBR). Subsequently, burning areas were analyzed using ΔNBR, as shown in Equation 4 (Smith *et al*., 2007).

$$NBR=(NIR-SWIR)/(NIR+SWIR) \quad (3)$$

Where:
NIR=Near-infrared (NIR) reflectance
SWIR=Shortwave-infrared (SWIR) reflectance

$$\Delta NBR=NBR\ pre\text{-}fire - NBR\ postfire \quad (4)$$

Where:
ΔNBR=NBR difference value
NBR pre-fire=NBR value before the fire
NBR postfire=NBR value after fire

Validity assessment

False color composite

A false-color composite was created to inspect the validity of burning areas caused by forest fires. Data obtained from Landsat 8 satellite were used for creating a false-color composite by mixing red, green, and blue wavelengths with SWIR NIR and Red (false color composite: 7(R),5(G),4(B)) wavelength. This kind of false color composite can show burning areas clearly with purple to dark purple in the manner of spreading from the center of a forest fire or the direction of active spreading shown with orange to red. Forest areas were shown with green, deciduous forest areas with light purple, pink, and white, and open areas with white, pink, or light orange. Water sources were shown with dark blue, and agricultural areas were shown with white, light green, or dark green based on types of appearance of plants and the density of cover crops (Uttaruk *et al*., 2022).

Random forest

Random forest is a machine-learning model developed from decision tree. Random forest adds the number of trees giving more efficiency and accuracy (Belgiu and Dragut, 2016; Deur *et al*., 2020). Currently, random forest is highly preferred (Phiri *et al*., 2018). The principle of random forest is building a model from various sub-models of decision trees. While performing prediction, each decision tree will perform predictions, and the prediction results can be calculated by voting output that is mainly selected by decision tree in case of classification or finding the mean from each decision tree's output in the case of regression (Pal, 2005). In this research, the sample size was calculated before sampling representatives of burning areas in the research area by using random points

through random forest in the ArcGIS program. Subsequently, data from sample groups were classified into two types: points of burning areas and non-burning areas for evaluating accuracy.

Consistency Test with Kappa

The Kappa coefficient, or Cohen's Kappa coefficient as it is officially known (Banko, 1998), is the statistic used for testing the consistency level in two data groups. In some cases, it may be used for comparing the evaluation of the same dataset from two evaluators. In comparison, the Kappa coefficient is not required to be based on the hypothesis that interested data were distributed using normal distribution or non-parametric statistics. Results obtained from the Kappa coefficient explained the consistency of the two datasets.

RESULTS AND DISCUSSION

Results of False Color Composite for Inspecting Burning Areas

Results of the analysis on burning areas caused by forest fires between 2017 and 2021 through data obtained from Landsat 8 satellite were used for creating false color composite by mixing colors in red, green, and blue wavelength with SWIR NIR and Red (false color composite: 7(R),5(G),4(B)) wavelength in pre-fire and postfire periods based on NBR and ΔNBR. Moreover, the accuracy of burning areas caused by forest fires was tested by using random points with 60 points. Analysis results are shown in Figure 2.

From Figure 2, it was found that false color composite 7(R),5(G),4(B) created from data obtained from Landsat 8 satellite for inspecting burning areas caused by forest fire was shown in purple to dark purple in the manner of spreading from the center of a forest fire or the direction of active fire's spreading that were shown with orange to red. Forest areas were shown with green. Deciduous forest areas were shown with light purple, pink, and white. Open areas were shown with white, pink, or light orange. Water sources were shown with dark blue, and agricultural areas were shown with white, light green, or dark green based on the types and appearance of plants and the density of cover crops.

Moreover, when analyzing the results of false color composite 7(R), 5(G), and 4(B) from Landsat 8 satellite data with ΔNBR through 60 random points, it was found that there were 49 points of 60 points of burning areas that were results of analysis on ΔNBR in 2017 calculated to be 81.66%.

Results of the analysis on ΔNBR in 2018 revealed that 49 points of 60 points of burning areas were calculated to be 81.66%. Results of the analysis on ΔNBR in 2019 revealed that there were 50 points out of 60 points of burning areas calculated to be 83.33%. Results of the analysis on ΔNBR in 2020 revealed that 49 points of 60 points of burning areas were calculated to be 81.66%. Results of the analysis on ΔNBR in 2021 revealed that there were 52 points out of 60 points of burning areas calculated to be 86.66%.

NBR pre-fire in 2017	NBR postfire in 2017	ΔNBR in 2017
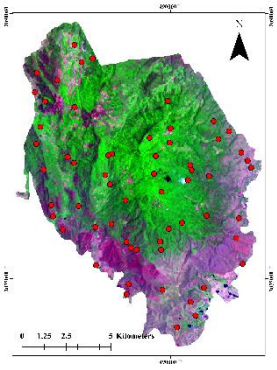	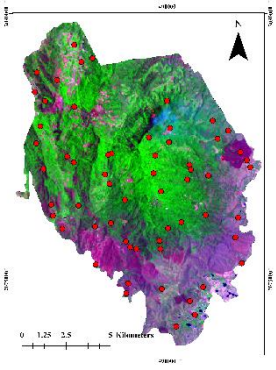	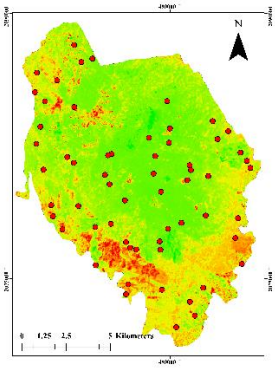
NBR pre-fire in 2018	NBR postfire in 2018	ΔNBR in 2018
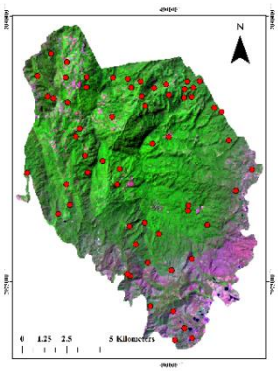	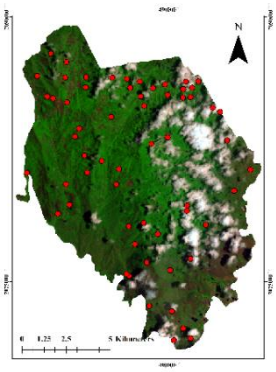	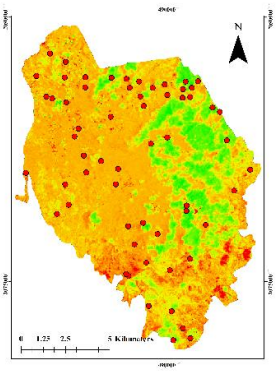
NBR pre-fire in 2019	NBR postfire in 2019	ΔNBR in 2019
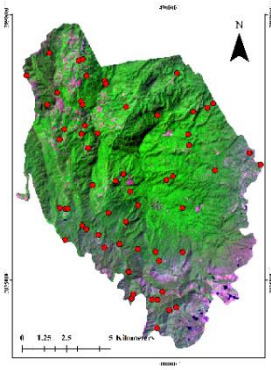	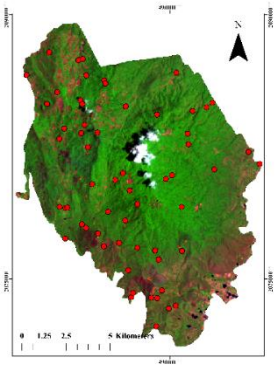	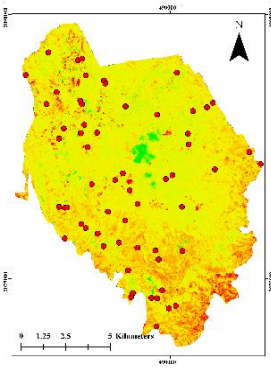
NBR pre-fire in 2020	NBR postfire in 2020	ΔNBR in 2020

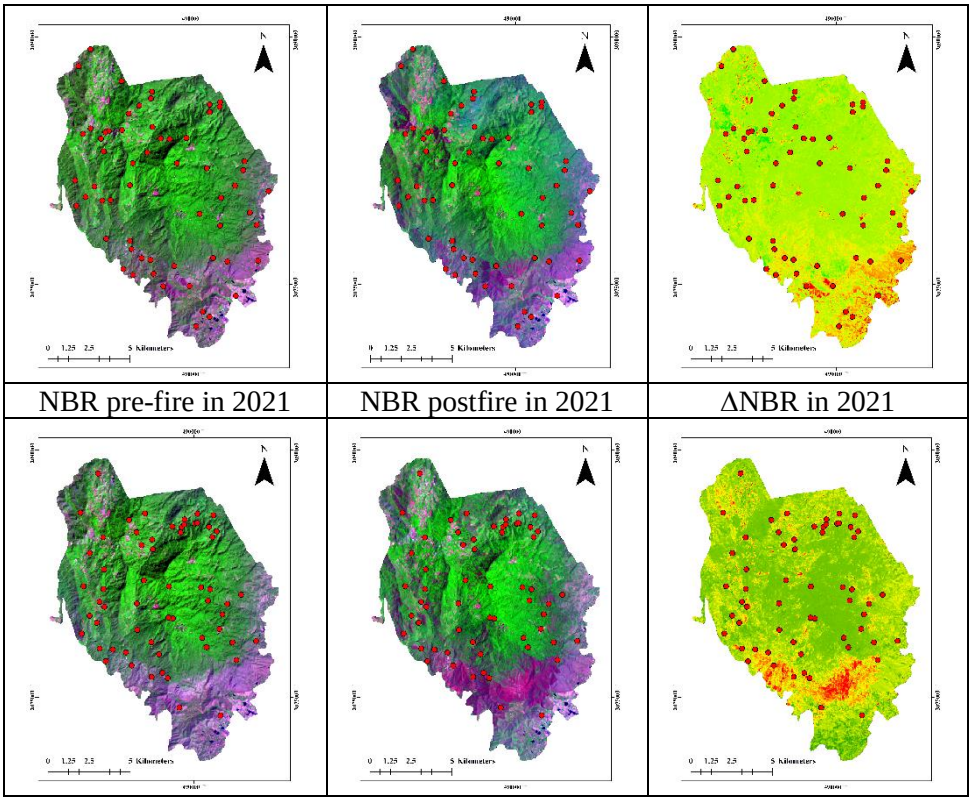

Figure 2. NBR pre-fire, NBR postfire, and ΔNBR between 2017 and 2021

Results of False Color Composite for Inspecting Burning Areas

In this research, results of analysis on data obtained from Landsat 8 satellite (false color composite) and ΔNBR between 2017 and 2021 were tested on consistency using Kappa. From a total of 60 random points, they were divided into 20 points of burning areas, 20 non-burning areas, and 20 forest areas. Random points were determined by creating random points in the ArcGIS program (Data Management Tools > Feature Class > Create Random Points) (ArcGIS Desktop, 2021) and comparing them with point-by-point by visual analysis. Results of the consistency test with Kappa are shown in Table 1.

From ΔNBR 2017 data, it was found that overall accuracy was 81.66%. It was also found that the Kappa coefficient was 0.78. When considering the class of the burning areas, it was found that the producer's accuracy was 73.91%, with an omission error of 26.09%, a user's accuracy of 85%, and commission error of 15%.

From ΔNBR 2018 data, it was found that overall accuracy was 81.66%. It was also found that the Kappa coefficient was 0.81. When considering the class of burning areas, it was found that the producer's accuracy was 78.94 %, with an omission error of 21.06%, a user's accuracy of 75%, and commission error of 25%.

Table 1. Consistency test with Kappa

ΔNBR in 2017					
ΔNBR	Forest area	Non-forest area	Burning area	Sum	User's accuracy
Forest area	**17**	1	2	20	85%
Non-forest area	1	**15**	4	20	75%
Burning area	1	2	**17**	20	85%
Sum	19	18	23	**60**	
Producer's accuracy	89.47%	83.33%	73.91%		
Kappa statistics	0.78				
ΔNBR in 2018					
ΔNBR	Forest area	Non-forest area	Burning area	Sum	User's accuracy
Forest area	**18**	1	1	20	90%
Non-forest area	1	**16**	3	20	80%
Burning area	3	2	**15**	20	75%
Sum	22	19	19	**60**	
Producer's accuracy	81.81%	84.21%	78.94%		
Kappa statistics	0.81				
ΔNBR in 2019					
ΔNBR	Forest area	Non-forest area	Burning area	Sum	User's accuracy
Forest area	**17**	2	1	20	85%
Non-forest area	2	**18**	0	20	90
Burning area	1	4	**15**	20	75%
Sum	20	24	16	**60**	
Producer's accuracy	85%	75	93.75%		
Kappa statistics	0.82				
ΔNBR in 2020					
ΔNBR	Forest area	Non-forest area	Burning area	Sum	User's accuracy
Forest area	**16**	1	3	20	80%
Non-forest area	5	**14**	1	20	70%
Burning area	0	1	**19**	20	95%
Sum	21	16	23	**60**	
Producer's accuracy	76.19%	87.5%	82.60%		
Kappa statistics	0.84				
ΔNBR in 2021					
ΔNBR	Forest area	Non-forest area	Burning area	Sum	User's accuracy
Forest area	**18**	0	2	20	90%
Non-forest area	1	**16**	3	20	80%
Burning area	0	2	**18**	20	90%
Sum	19	18	23	**60**	
Producer's accuracy	94.73%	88.88%	78.26%		
Kappa statistics	0.82				

From ΔNBR 2019 data, it was found that overall accuracy was 83.33%, and it was also found that the Kappa coefficient was 0.82. When considering the class of burning areas, it was found that the producer's accuracy was 93.75%, with an omission error of 6.25%, a user's accuracy of 75%, and a commission error of 25%.

From ΔNBR 2020 data, it was found that overall accuracy was 81.66%. It was also found that the Kappa coefficient was 0.84. When considering the class of burning areas, it was found that the producer's accuracy was 82.60%, with an omission error of 17.40%, a user's accuracy of 95%, and commission error of 5%.

From ΔNBR 2021 data 2022, it was found that overall accuracy was 86.66%. It was also found that the Kappa coefficient was 0.82. When considering the class of burning areas, it was found that the producer's accuracy was 78.26%, with an omission error of 21.74%, a user's accuracy of 90%, and commission error of 5%.

The burning index that uses 2 data periods before and after the burning area is analyzed, such as the ΔNBR index, provides the results of the analysis of the burning area that is more accurate than using data at a single period to calculate. Schepers *et al.* (2014) and Liu *et al*. (2020) concluded that the burning index was used from satellite images recorded during the visible and near-infrared waves. Intense than the combustion index that uses the near-infrared wave with middle infrared. In addition, the accuracy of the analysis of the combustion area depends on the selection of the index that uses the wave range to analyze the appropriate combustion space, with the time of the analyzed data must be appropriate as well.

However, if the rehabilitation of the burned area, there should be a distance between the data that is analyzed and compared with the NBR and the ΔNBR index and, therefore, should be more than one year apart because it will be able to monitor the rehabilitation, including the violence of combustion. In addition, this study is in line with the research on "A New Metric for Quantifying Burn Severity: The Relativized Burn Ratio" (Parks *et al*., 2014), the study "Evaluation of Spectral Indices for Assessing Fire Severity in Australian Temperate Forests" (Tran *et al.*, 2018), and The study "Evaluating the Differenced Normalized Burn Ratio for Assessing Fire Severity Using Sentinel-2 Imagery in Northeast Siberian Larch Forests" (Delcourt *et al.*, 2021), concluded that NBR and ΔNBR can identify burning areas caused by forest fire effectively.

CONCLUSIONS

Usually, in the event of any combustion caused by any cause, poor management or control may lead to spreading. After burning, the soil's color will be changed to grey or even black due to heat on the soil caused by the burning of leaves or scraps from harvesting crops that covers the soil. After burning, these fuels will leave black soot and ashes. If satellite data are used for inspecting areas after the scene, burned areas will be able to be visually observed and separated more clearly. However, visual interpretation may be insufficient to survey and

inspect for assess damages because each wildfire can cause massive damage. As a result, researchers and related persons often use data from aerial photography or satellite to inspect or assess initial damages. This research aims to apply Normalized Burn Ratio (NBR), and Difference Normalized Burn Ratio (ΔNBR) because many researchers have applied them to analyze burned areas via satellite data. Normalized Burn Ratio, or NBR, was designed to focus on burned areas, and its calculation was similar to that of the Normalized Difference Vegetation Index (NDVI). However, NBR uses Nir Infrared (NIR) and Short Wave Infrared (SWIR) because plentiful plants will have a high reflection in NIR wavelength, but its reflection will be low in SWIR wavelength. Therefore, we can separate burned areas from other areas correctly.

This research was conducted to inspect burning areas caused by forest fires in the national park through data obtained from Landsat 8 satellite and Normalized Burn Ratio in the area of Doi Suthep-Pui National Park in Muang Chiang Mai District, Mae Rin District, and Hang Dong District in Chiang Mai province during 2018–2021. The study concluded that data from Landsat 8 satellite and Normalized Burn Ratio could specify burning areas that occurred in the research area and false color composite 7(R), 5(G), 4(B), NBR, and ΔNBR from data obtained from Landsat 8 satellite could represent burning areas. Moreover, results of the consistency test with Kappa between 2018 and 2021 revealed high accuracy, with an overall accuracy of 81.66%, 81.66%, 83.33%, 81.66%, and 86.66%, respectively. In addition, it was also found that the Kappa coefficient was 0.78, 0.81, 0.82, 0.82, and 0.84, respectively. Anyone interested and related agencies could efficiently apply this method to inspect further burning areas caused by forest fires.

ACKNOWLEDGEMENTS

This research project is financially supported by Mahasarakham University.

REFERENCES

ArcGIS Desktop. (2021). Create random points. Available online: https://desktop.arcgis.com/en/arcmap/latest/tools/data-management-toolbox/create-random-points.htm (accessed on 15 March 2023).

Baankluayonline. (2020). Impact of Forest Fires. Available online: http://www.baankluayonline.co/infographic-about-forest-fire/ (accessed on 16 March 2023).

Banko, G. (1998). A Review of Assessing the Accuracy of Classifications of Remotely Sensed Data and of Methods Including Remote Sensing Data in Forest Inventory. RePEc: Research Papers in Economics. http://pure.iiasa.ac. at/id/eprint/5570/

Belgiu, M., & Drăguţ, L. (2016). Random forest in remote sensing: A review of applications and future directions. ISPRS Journal of Photogrammetry and Remote Sensing, 114, 24–31. https://doi.org/10.1016/j.isprsjprs.2016.01.011

Boer, M. M., Sadler, R., Wittkuhn, R. S., McCaw, W. L., & Grierson, P. F. (2009). Long-term impacts of prescribed burning on regional extent and incidence of wildfires—Evidence from 50 years of active fire management in SW Australian forests. Forest Ecology and Management, 259(1), 132–142. https://doi.org/10.1016/j.foreco.2009.10.005

Chiang Mai Provincial Office. (2021). Briefing Chiang Mai Province. Available online: https:// www.chiangmai.go.th/managing/public/D8/8D12Nov2020103 220.pdf. (accessed on 20 March 2022).

Debbarma, J., & Debnath, J. (2021). Assessment on the impact of the Tripura earthquake (January 3, 2017, mw = 5.6) in Northeast India. Journal of the Geographical Institute "Jovan Cvijić" SASA, 71(1), 1–13. DOI: 10.2298/IJ GI2101001D.

Delcourt, C. J. F., Combee, A., Izbicki, B., Mack, M. C., Maximov, T., Petrov, R., Rogers, B. M., Scholten, R. C., Shestakova, T. A., van Wees, D., & Veraverbeke, S. (2021). Evaluating the Differenced Normalized Burn Ratio for Assessing Fire Severity Using Sentinel-2 Imagery in Northeast Siberian Larch Forests. Remote Sensing, 13(12), 2311. DOI: 10.3390/rs13122311

Department of National Parks, Wildlife and Plant Conservation. (n.d.). Policies and Ideas for Solving Forest Fire Problems. Available online: https://www.dnp.go.th/forestfire/firescience/lesson%202/lesson21.htm/ (accessed on 17 March 2023).

Deur, M., Gašparović, M., Balenović, I. (2020). Tree Species Classification in Mixed Deciduous Forests Using Very High Spatial Resolution Satellite Imagery and Machine Learning Methods. Remote Sensing, 12(23), 3926. DOI: 10.3390/rs12233926

Elachi, C., & Zyl, J.V. (2021). Introduction to the Physics and Techniques of Remote Sensing (3rd Edition). John Wiley & Sons, Inc. DOI: 10.1002/9781119523048

ESA. (2016). Physics of Remote Sensing. Available online: https://earth.esa.int/ web/eo-summer-school/documents/973910/2642313/JG1to3.pdf (accessed on 25 March 2022).

Flannigan, M. D., Stocks, B. J., & Wotton, B. M. (2000). Climate change and forest fires. The Science of the Total Environment, 262(3), 221–229. DOI:10.1016/S0048-9697(00)00524-6

Gnews. (n.d.). Forest Fire Prevention. Available online: https://gnews.apps.go.th/news?news=13409 (accessed on 27 March 2022).

Jomsrekrayom, N., Meena, P., & Laosuwan, T. (2021). Spatiotemporal Analysis of Vegetation Drought Variability in the Middle of the Northeast Region of Thailand using Terra/Modis Satellite Data. Geographia Technica, 16(Special Issue), 70–81. DOI: 10.21163/GT_2021.163.06

Keeley, J. E. (2009). Fire intensity, fire severity and burn severity: A brief review and suggested usage. International Journal of Wildland Fire, 18(1), 116–126.

Kongmeesup, I. (2020). Interactions between Climate Change and the World's Forest Sector. Naresuan Agricultural Journal, 17(2), 1–19.

Laosuwan, T., Sangpradid, A., Gomasathit, T., & Rotjanakusol, T. (2016). Application of remote sensing technology for drought monitoring in Mahasarakham Province, Thailand. International Journal of Geoinformatics, 12(3), 17–25.

Linta, N., Mahavik, N., Chatsudarat, S., Seejata K., & Yodying A. (2021). Analysis of Burning Area from Forest Fire using Sentinel-2 Image: A Case Study of Pai, Mae Hong Son Province. Journal of Applied Informatics and Technology, 3(2), 101–121.

Liu, S., Yongjie Zheng, Michele Dalponte, M., & Tong, X. (2020) A novel fire index-based burned area change detection approach using Landsat-8 OLI data, European Journal of Remote Sensing, 53:1, 104–112, DOI: 10.1080/ 22797254.2020.1738900

Mohammadi, F., Bavaghar, M.P., & Shabanian N. (2014). Forest Fire Risk Zone Modeling Using Logistic Regression and GIS: An Iranian Case Study. Small-scale Forestry, 13, 117–125.

Pal, M. (2005). Random Forest Classifier for Remote Sensing Classification. International Journal of Remote Sensing, 26(1), 217–222.

Panyakam, M., & Pongsawat, P. (2022). The Evolution of Wildfire and Haze Policies: A Case study of Wildfire and Haze Policies in Chiang Mai. Governance Journal, 10(1), 408-446.

Parks, S., Dillon, G., & Miller, C. (2014). A New Metric for Quantifying Burn Severity: The Relativized Burn Ratio. Remote Sensing, 6(3), 1827–1844. https://doi.org/10.3390/rs6031827

Phiri, D., Morgenroth, J., Xu, C., & Hermosilla, T. (2018): Effects of pre-processing methods on Landsat OLI-8 land cover classification using OBIA and random forests classifier, International Journal of Applied Earth Observation and Geoinformation, 73, 170–178. DOI: 10.1016/j.jag.2018.06. 014.

Potić, I. M., Ćurčić, N. B., Radovanović, M. M., Stanojević, G. B., Malinović-Milićević, S. B., Yamashkin, S. A., & Yamashkin, A. A. (2021). Estimation of Soil Erosion Dynamics using Remote Sensing and SWAT in Kopaonik National Park, Serbia Journal of the Geographical Institute "Jovan Cvijić" SASA, 71(3), 231–247. DOI: 10.2298/IJGI2103231P

Prohmdirek, T., Chunpang, P., & Laosuwan, T. (2020). The relationship between normalized difference vegetation index and canopy temperature that affects the urban heat island phenomenon. Geographia Technica, 15(2), 222–234. DOI: 10.21163/GT_2020.152.21

Rotjanakusol, T., & Laosuwan, T. (2018a). Inundation Area Investigation Approach using Remote Sensing Technology on 2017 Flooding in Sakon Nakhon Province Thailand. Studia Universitatis Vasile Goldis Arad, Seria Stiintele Vietii, 28(4), 159–166.

Rotjanakusol, T., & Laosuwan, T. (2018b). Estimation of land surface temperature using Landsat satellite data: A case study of Mueang Maha Sarakham District, Maha Sarakham Province, Thailand for the years 2006 and 2015. Scientific Review Engineering and Environmental Sciences, 27(4), 401–409. DOI 10.22630/PNIKS.2018.27.4.39

Rotjanakusol, T., & Laosuwan, T. (2019). An Investigation of Drought around Chi Watershed during Ten-year Period using Terra/Modis Data. Geographia Technica, 14(2), 74–83. DOI: 10.21163/GT_2019.142.07

Royal Forest Department. (n.d.). Types of Wildfires. Available online: http://old.forest.go.th/forestprotect/images/stories/Types%20of%20forest% 20fire3.pdf (accessed on 27 March 2022).

Ruthamnong S. (2019). Burned area extraction using Multitemporal Difference of Spectral Indices from Landsat 8 Data: A case study of Khlong Wang Chao, Klong Lan and Mae Wong National Park. The Golden Teak: Humanity and Social Science Journal, 25 (2), 49–65.

Sangpradid, S., Uttaruk, Y.,Rotjanakusol, T., Laosuwan T. (2021): Forecasting time series change of the average enhanced vegetation index to monitoring drought condition by using terra/modis data. Agriculture and Forestry, 67 (4): 115-129. DOI:10.17707/AgricultForest.67.4.10

Schepers, L., Haest, B., Veraverbeke, S., Spanhove, T., Vanden Borre, J., & Goossens, R. (2014). Burned Area Detection and Burn Severity Assessment of a Heathland Fire in Belgium Using Airborne Imaging Spectroscopy (APEX). Remote Sensing, 6(3), 1803–1826. https://doi.org/10.3390/rs6031 803.

Smith, A. M. S., Lentile, L. B., Hudak, A. T. & Morgan, P. (2007). Evaluation of linear spectral unmixing and ΔNBR for predicting post- fire recovery in a North American ponderosa pine forest, International Journal of Remote Sensing, 28(22), 5159–5166. DOI: 10.1080/01431160701395161

Suriya, W., Chunpang, P., & Laosuwan, T. (2021). Patterns of relationship between PM10 from air monitoring quality station and AOT data from MODIS sensor onboard of Terra satellite. Scientific Review Engineering and Environmental Sciences, 30(2), 236–249. DOI 10.22630/PNIKS.2021.30.2. 20

Tariq, A., Shu, H., LI Q., Altan, O., Khan, M.R., Baqa, M.F., & Lu, L. (2021a). Quantitative Analysis of Forest Fires in Southeastern Australia Using SAR Data. Remote Sensing, 13(12), 2386, DOI: 10.3390/rs13122386

Tariq A., Shu H., Gagnon A.S., Li Q., Mumtaz F., Hysa A., Siddique M.A., & Munir I. (2021b). Assessing Burned Areas in Wildfires and Prescribed Fires with Spectral Indices and SAR Images in the Margalla Hills of Pakistan, Forests, 12(10), 1371. DOI: 10.3390/f12101371

Thangaraj, K., & Karthikeyan, S. (2021). Assessment of Shoreline Positional Uncertainty using Remote Sensing and GIS Techniques: A Case Study from the East Coast of India. Journal of the Geographical Institute "Jovan Cvijić" SASA, 71(3), 249–263. DOI: 10.2298/IJGI2103249T

Thai National Parks. (2023). Doi Suthep-Pui National Park. Available online: https://www.thainationalparks.com/doi-suthep-pui-national-park (accessed on 25 March 2022).

Tran, B., Tanase, M., Bennett, L., & Aponte, C. (2018). Evaluation of Spectral Indices for Assessing Fire Severity in Australian Temperate Forests. Remote Sensing, 10(11), 1680. DOI: 10.3390/rs10111680

University of Lucknow. (n.d.). Physics of Remote Sensing. Available online: https://www.lkouniv.ac.in/site/writereaddata/siteContent/202004021910156 883ajay_misra_geo_principles_of_RS.pdf (accessed on 29 May 2023).

Untamedscience. (n.d.). The Environmental Impact of Forest Fires. Available online: https://untamedscience.com/blog/the-environmental-impact-of-forest-fires/. (accessed on 29 May 2023).

Urbancreature. (2021). Northern Forest Fire. Available online: https:// urbancreature.co/greenindex-wildfire/ (accessed on 29 May 2023).

Uttaruk, Y., Laosuwan, T. (2020). Methods of estımatıon for above ground carbon stock ın Nongbua-nonmee communıty forest, Maha Sarakham Provınce, Thaıland. Agriculture and Forestry, 66 (3), 183-195. DOI: 10.17707/AgricultForest.66.3.15

Uttaruk, Y., Rotjanakusol, T., & Laosuwan, T. (2022). Burned Area Evaluation Method for Wildfires in Wildlife Sanctuaries Based on Data from Sentinel-2 Satellite. Polish Journal of Environmental Studies, 31(6), 1-11. https://doi.org/10.15244/pjoes/152835

USGS. (2022). Landsat 8. Available online: https://www.usgs.gov/landsat-missions/landsat-8. (accessed on accessed on 29 May 2023).

3armyarea-rta. (n.d.). Solution to Forest Fire Problem. Available online: http:// www.3armyarea-rta.com/ pdf/haze.pdf/ (accessed on 29 May 2023).